第 50 卷第 11 期 中国科学技术大学学报 Vol. 50, No. 11
2020 年 11 月 JOURNAL OF UNIVERSITY OF SCIENCE AND TECHNOLOGY OF CHINA Nov. 2020
Received：2020-09-15；Revised：2020-11-23 doi:10.3969/j.issn.0253-2778.2020.11.007

An analogical model for tympanometry of the pathological human middle ear

LI Mugeng, CHEN Lin*
Hefei National Laboratory for Physical Sciences at the Microscale, University of Science and Technology of China, Hefei 230027, China
*Corresponding author：linchen@ustc.edu.cn

Abstract：Tympanometry involves measuring the acoustic admittance of the middle ear system as a function of air pressure in the external auditory meatus. Since tympanogram provides a noninvasive and objective evaluation of middle ear functions, it has gained a wide application in the ear, nose, and throat (ENT) clinic. In this study, parameters of the middle ear circuit analog model were manipulated to mimic tympanograms of the ear with a flaccid eardrum and otosclerosis, which were consistent with those typically observed in the clinic. Also, the recently developed inner ear model was combined with the classical middle ear model to mimic tympanograms of the ear with a flaccid eardrum. Applying the circuit model to different middle ear diseases can provide a better understanding of the mechanism of tympanometry and promote its clinical utility.

Keywords：middle ear; tympanometry; otosclerosis; middle ear electroacoustic model
CLC number：R764.5 **Document code**：A

1 Introduction

Tympanometry involves measuring the acoustic admittance (Y), acoustic conductance (G) and acoustic susceptance (B) of the middle ear system with various air pressures in the external auditory meatus, which can help diagnose middle ear diseases, such as otosclerosis, ossicular discontinuities and atrophy of the tympanic membrane. Since tympanometry provides a rapid, noninvasive and objective approach to the evaluation of middle ear functions, it has gained a wide application in the ear, nose, and throat (ENT) clinic[1]. Traditionally, tympanograms are measured only with a low-frequency probe tone (e.g., 226 Hz) and are typically bell-shaped. With the development of new technology, high-frequency probe tones are more and more used in tympanometry (e.g., 678 Hz and 1000 Hz) and now newer multifrequency and wideband immittance systems are commercially available[2]. Although these new technologies can provide more information on middle ear diseases, the shapes of tympanograms measured with multiple probe frequencies which become notched at higher frequencies are complicated in contrast to a simple bell-shape[3, 4]. Vanhuyse et al. correlated the morphology of admittance tympanograms with the impedance of the middle ear as functions of air pressure in the external auditory meatus to interpret the complicated shapes[5]. Zwislocki developed an electroacoustic analog model to represent the middle ear with zero pressure in the ear canal[6]. In subsequent studies, different investigators improved Zwislocki's circuit model to calculate the acoustic immittance of the middle ear[7, 8]. Based on the Zwislocki's eletroacoustic analog, Chen and Shen developed a model describing the ear canal with the acoustic theory of a tube. Tympanograms of different patterns for the normal ear were reproduced with the model and were in agreement with experimental observations reported by other investigators and the Vanhuyse theory[1].

Jerger proposed a system which was most widely utilized for classifying 226 Hz tympanograms[9]. Tympanograms were categorized into a reasonably small number of types according to their configurations found clinically, such as type A, type A_s, type A_D, type B and type C. Type A tympanograms have a distinctive peak occurring near atmospheric pressure and are typical of normal people. If the type A tympanogram has a greatly reduced peak, it will be classified as type A_s, which is generally associated with otosclerosis. In contrast, if the type A tympanogram has a greatly increased peak height, it will be classified as type A_D, which is generally associated with scarred or flaccid eardrums. In most cases, type A_s is related to middle ear diseases that could increase stiffness, while type A_D is related to those

Citation：LI Mugeng, CHEN Lin. An analogical model for tympanometry of the pathological human middle ear. J. Univ. Sci. Tech. China, 2020, 50(11): 1431-1439.

that could decrease stiffness[10]. However, a theoretical analysis of the effects caused by middle ear diseases is needed for people to understand different types of tympanograms more deeply.

In the present study, we used a theoretical model to analyze different types of tympanograms under conditions of different middle ear diseases such as otosclerosis and atrophy of tympanic membrane. The model parameters were manipulated to simulate changes in acoustic properties of middle ear elements under conditions of different middle ear diseases. The validity of the model was evaluated by comparing the tympanograms from the model with those actually recorded from the human ear.

2 Model and parameters

Fig. 1 shows the block diagram of the acoustic units of the middle ear proposed by Zwislocki[5]:

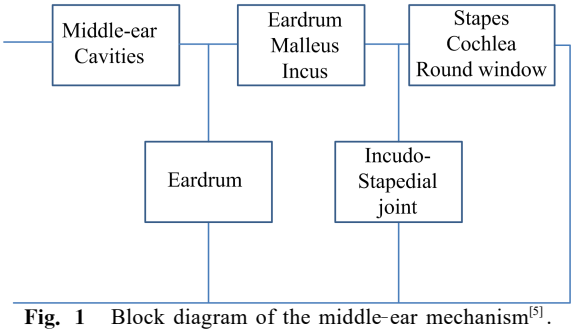

Fig. 1 Block diagram of the middle-ear mechanism[5].

Fig. 2 shows the improved model structure proposed by Chen and Shen for simulating tympanograms of the normal ear, which considered contributions from both the ear canal and the middle ear[1]:

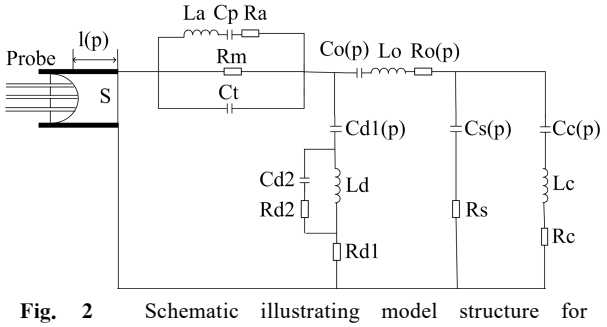

Fig. 2 Schematic illustrating model structure for simulating tympanograms of the normal ear.

The impedance Z_1 at the probe tip is given by[11]:

$$Z_1 = \alpha \frac{R + j(X + \alpha\beta)}{\alpha - \beta X + j\beta R} \tag{1}$$

where $\alpha = \sigma c/S$, σ is the density of the medium (g/cm^3), c is the sound speed (cm/s), S is the cross-section area of the ear canal (cm^2), $\beta = \tan(kl)$, l is the average distance between the probe tip and the tympanic membrane (cm), $k = 2\pi\upsilon/c$, ν is the probe frequency (Hz), R is the resistance of the middle ear at the tympanic membrane(Ω); X is the reactance of the middle ear at the tympanic membrane. The value of c was set to 34000 cm/s, and the value of S was set to 0.48 cm^2. The impedance Z_1 can be converted into admittance and then expressed as conductance G_1 and susceptance B_1 at the probe, which are actually altered by ear-canal pressure[1]:

$$G_1(p) = \frac{[1 + \beta^2(p)]R(p)}{[X(p) + \alpha\beta(p)]^2 + R^2(p)} \tag{2}$$

$$B_1(p) = \frac{\beta(p)}{\alpha} - \frac{[1 + \beta^2(p)][X(p) + \alpha\beta(p)]}{[X(p) + \alpha\beta(p)]^2 + R^2(p)} \tag{3}$$

To determine the variation of $G_1(p)$ and $B_1(p)$ with ear-canal pressure p, Chen and Shen also assumed that analog elements l, $Cd1$, Co, Cs, Cc and Ro as functions of ear-canal pressure p were represented by the following equations[1]:

$$l(p) = 1.45 + 0.123(1 - e^{-|p|/200}),\ p \geqslant 0 \tag{4}$$

$$l(p) = 1.45 - 0.123(1 - e^{-|p|/200}),\ p < 0 \tag{5}$$

$$Cd1(p) = Cd1(T_0 + T_1{}^{-|p|/T_2}) \tag{6}$$

$$Co(p) = Co(T_0 + T_1 e^{-|p|/T_2}) \tag{7}$$

$$Cs(p) = Cs(T_0 + T_1 e^{-|p|/T_2}) \tag{8}$$

$$Cc(p) = Cc(T_0 + T_1 e^{-|p|/T_2}) \tag{9}$$

$$Ro(p) = Ro(T_0 + T_1 e^{-|p|/T_2}),\ p \geqslant 0 \tag{10}$$

$$Ro(p) = Ro(T_0 - T_1 e^{-|p|/T_2}),\ p < 0 \tag{11}$$

where p is ear-canal pressure; T_0, T_1 and T_2 are constants [1]. For simulating different kinds of tympanograms, values selected for the model parameters are listed in Tabs. 1, 2 and 3.

Tab. 1 Values selected for constants T_0, T_1 and T_2 in Eqs. (6)～(11) for simulating tympanograms.

Element	Eqs.	T_0	T_1	T_2
$Cd1(p)$	(6)	0.05	0.95	50
$Co(p)$	(7)	0.05	0.95	20
$Cs(p)$	(8)	0.10	0.90	20
$Cc(p)$	(9)	0.20	0.80	20
$Ro(p)$, $p \geqslant 0$	(10)	0.15	0.85	15
$Ro(p)$, $p < 0$	(11)	1.75	0.75	25

Tab. 2 Parameter values selected for simulating type A, type A_D, type A_S and type C tympanograms at 226 Hz.

Element	Type A	Type A_D	Type A_s	Type C	Unit
Ra	10	10	10	10	Ω
La	14	14	14	14	mH
Cp	5.1	5.1	5.1	5.1	μF
Rm	500	500	500	500	Ω
Ct	0.35	0.35	0.35	0.35	μF
$Rd1$	200	200	200	200	Ω
$Cd1$	0.299	2.691	0.039	0.598	μF

Tab. 2 Parameter values selected for simulating type A, type A_D, type A_S and type C tympanograms at 226 Hz(continued).

Element	Type A	Type A_D	Type A_s	Type C	Unit
*Rd*2	220	220	220	220	Ω
*Cd*2	0.4	0.4	0.4	0.4	μF
Ld	45	45	45	45	mH
Ro	245	245	245	245	Ω
Lo	40	40	40	40	mH
Co	1.4	12.6	0.182	2.8	μF
Rs	3000	3000	3000	3000	Ω
Cs	0.25	2.25	0.0325	0.50	μF
Rc	550	550	550	550	Ω
Lc	20	20	20	20	mH
Cc	0.6	5.4	0.078	1.2	μF

Tab. 3 Parameter values selected for simulating tympanograms of the normal ear, the ear with a flaccid eardrum and the otosclerotic ear.

Element	Normal	Flaccid eardrum	Otosclerosis	Unit
Ra	10	10	10	Ω
La	14	24	14	mH
Cp	5.1	5.1	5.1	μF
Rm	500	50	500	Ω
Ct	0.35	0.35	0.35	μF
*Rd*1	200	10	200	Ω
*Cd*1	0.299	0.99	0.158	μF
*Rd*2	220	10	220	Ω
*Cd*2	0.4	0.8	0.212	μF
Ld	45	24.8	45	mH
Ro	245	245	245	Ω
Lo	40	80	40	mH
Co	1.4	2.8	0.742	μF
Rs	3000	400	3000	Ω
Cs	0.25	0.25	0.133	μF
Rc	550	20		Ω
Lc	20	20		mH
Cc	0.6	0.6		μF

3 Results

3.1 Simulation of different types of 226 Hz tympanograms

The model parameters were manipulated to simulate changes in acoustic properties of middle ear elements under conditions of different middle ear diseases. Different types of tympanograms measured with a 226 Hz probe tone were simulated with different parameters. Fig. 3 shows the simulated results of type A, type A_D, type A_S and type C tympanograms. Values selected for model parameters are listed in Tabs. 1 and 2. The type A tympanogram has a distinctive peak with a normal peak height in the vicinity of atmospheric pressure. The type A_D tympanogram has a very high peak, whereas the type A_S tympanogram has a very shallow peak. The type C tympanogram is single peaked at negative middle ear pressure (-200 daPa in Fig. 3) and is generally associated with Eustachian tube disorders. It is not difficult to find the general agreement of the simulated tympanograms with the typical clinical tympanograms[9].

3.2 Simulation of tympanograms from an ear with a flaccid eardrum

In an ear that has a flaccid eardrum, decreased stiffness and increased compliance can occur. The left panels of Fig. 4 show the tympanograms recorded at 226 and 678 Hz from a human ear with a flaccid eardrum reported by Shanks and Shelton[12]. Both conductance (G) and susceptance (B) tympanograms are single peaked at 226 Hz. At 678 Hz, the conductance (G) tympanogram is single peaked with an abnormally increased amplitude while the susceptance (B) tympanogram becomes notched and asymmetrical to the vertical axis. The right panels of Fig. 4 show the results calculated from the model simulating the tympanograms from the ear with a flaccid eardrum. Values selected for the model parameters are listed in Tabs. 1 and 3. It is evident from Fig. 4 that the model results are in good agreement with the experimental results.

3.3 Simulation of tympanograms from an otosclerotic ear

In the otosclerotic ear, the stape is immobilized in the

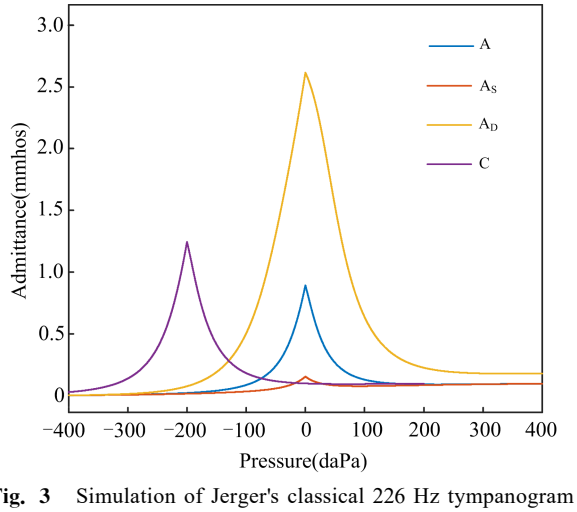

Fig. 3 Simulation of Jerger's classical 226 Hz tympanogram types[9].

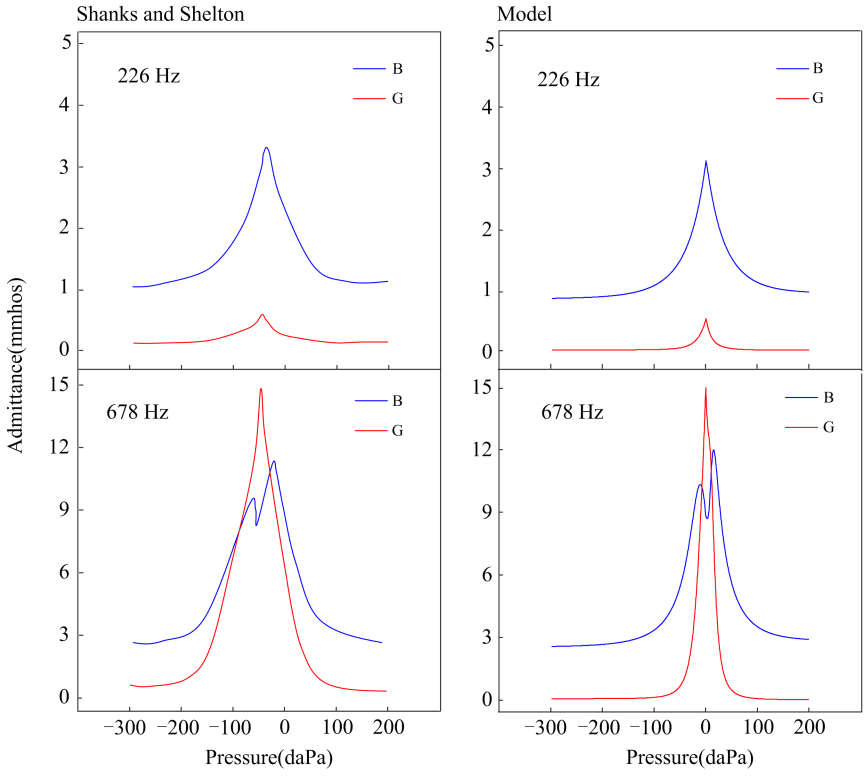

Fig. 4 Conductance (G) and susceptance (B) tympanograms from a human ear with a flaccid eardrum (redrawn from Ref.[12]) and from model.

oval window and the cochlea disconnected from the middle-ear system[13]. To simulate pathological tympanograms recorded from the ear with otosclerosis, the model structure was modified according to Zwislocki[6] and is illustrated in Fig. 5.

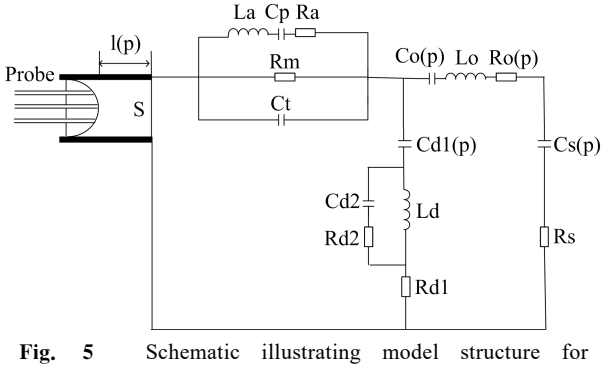

Fig. 5 Schematic illustrating model structure for simulating tympanograms of the ear with otosclerosis.

Values selected for the model parameters are listed in Tabs. 1 and 3. The upper panel of Fig. 6 shows a series of conductance (G) and susceptance (B) tympanograms from 226 to 1243 Hz from a human ear with otosclerosis reported by Shanks and Shelton[12]. The conductance (G) tympanograms are single peaked at all frequencies. The susceptance (B) tympanograms are single peaked at low frequencies while they become notched at high frequencies. The bottom panel of Fig. 6 shows the output of the model. It is not difficult to find the general agreement of the model results with the experimental results. Both the experimental results and model results show that the susceptance (B) tympanograms begin to notch at 1130 Hz.

Fig. 7 shows the model predictions of the susceptance (B) of a normal middle ear and an otosclerotic middle ear for zero ear-canal pressure as functions of frequency from 200 to 2000 Hz, which were calculated by assuming ear-canal length $l(p) = 0$. The model results have demonstrated that otosclerosis results in a higher resonant frequency of the middle ear (the frequency when the susceptance B=0) than that of the normal, which is consistent with experimental observations[3,14,15].

3.4 Combination of the new and classical models

Researchers have developed various models to study the impedances of the middle ear system[16-21]. O'Connor and Puria represented the tympanic membrane as a distributed parameter transmission line to solve the problem that the lumped parameter model representations for the tympanic membrane are not satisfactory at high frequencies (above 8 kHz)[17]. However, in the present study, the tympanograms we simulated were at a frequency lower than 2 kHz. The lumped parameter model representations for the tympanic membrane have been successful at low

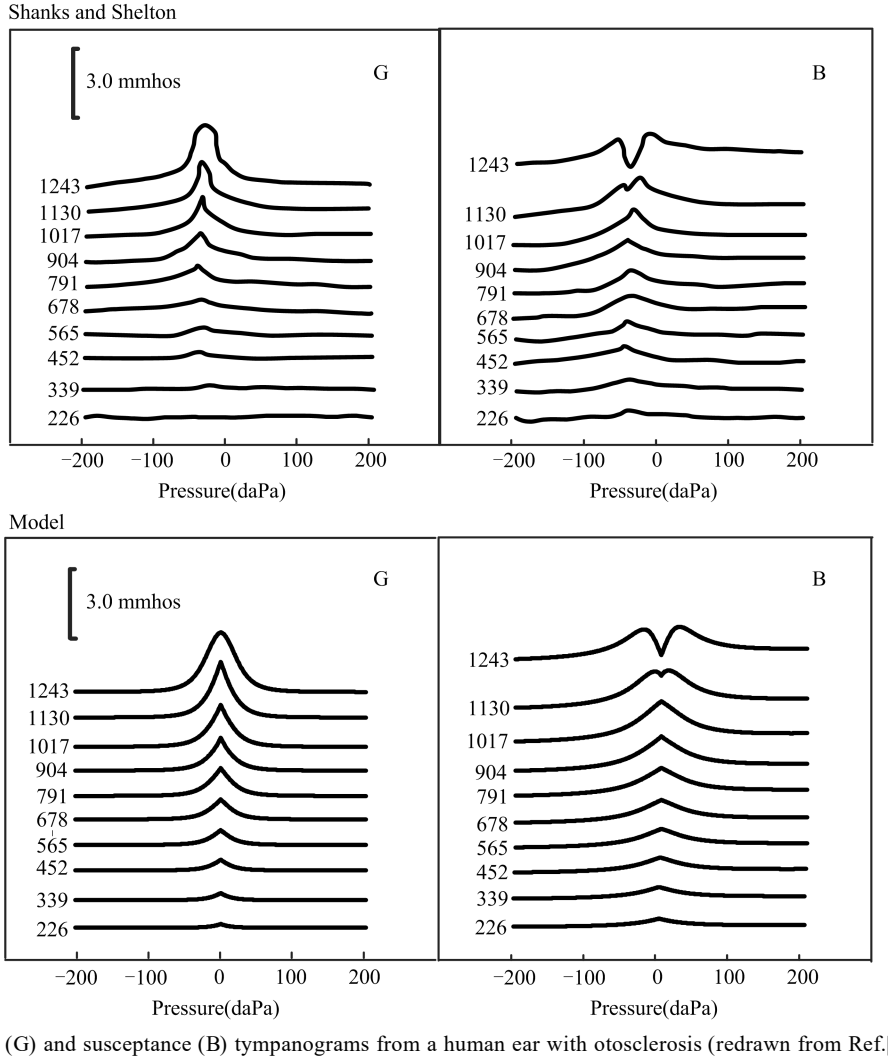

Fig. 6 Conductance (G) and susceptance (B) tympanograms from a human ear with otosclerosis (redrawn from Ref.[12]) and from model.

frequencies (below 6～8 kHz)[6,16,17].

Elliott et al.and Frear et al. investigated the acoustic impedances of the inner ear in a frequency range from 100 to 2000 Hz[18,19], corresponding to the frequencies in the present study. We combined Chen and Shen's model with their inner ear model (Fig. 8 and Tab. 4) to simulate the tympanograms of the ear with a flaccid eardrum. In the otosclerotic ear, the stape is immobilized in the oval window, and the cochlea disconnected from the middle ear system[6]. As a consequence, the simulated tympanograms of an otosclerotic ear with the combined model is the same as those with Chen and Shen's model (Fig. 5).

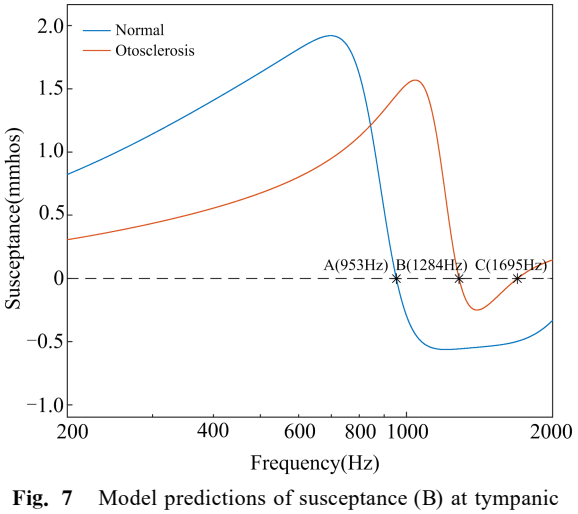

Fig. 7 Model predictions of susceptance (B) at tympanic membrane as functions of probe frequencies for zero canal pressures.

Fig. 9 shows the results calculated from Chen and Shen's model and the combined model simulating the tympanograms of the ear with a flaccid eardrum. There is a general agreement of the results from the combined model with those from Chen and Shen's model, indicating that the combination of Chen and Shen's model and the inner ear model is reasonable.

3.5 Simulation of the otosclerotic ear

Otosclerosis is caused by abnormal growth of bone near the stapes footplate, which can result in fixation of the

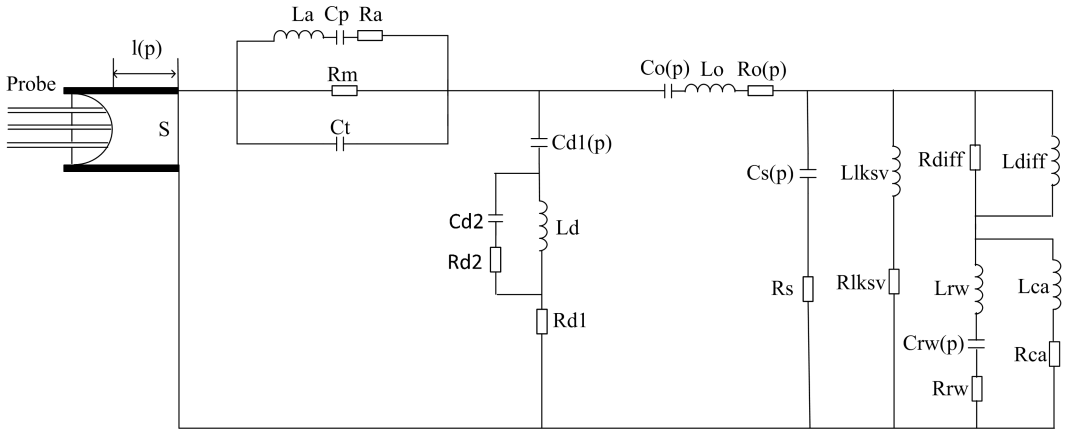

Fig. 8 Combined model structure for simulating tympanograms of the ear with a flaccid eardrum.

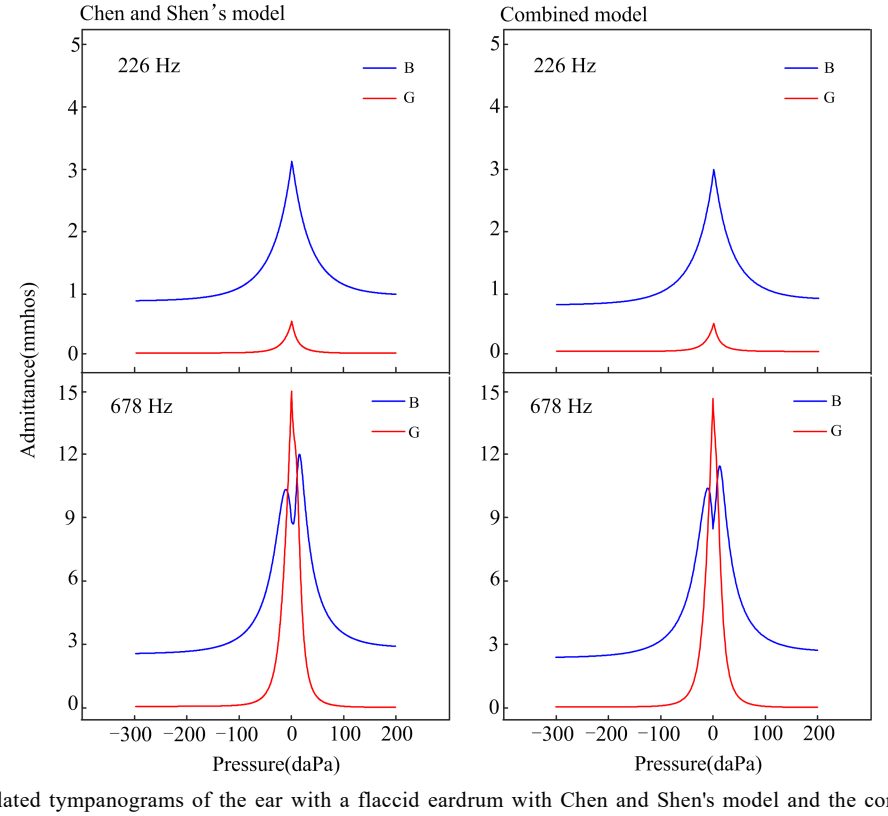

Fig. 9 Simulated tympanograms of the ear with a flaccid eardrum with Chen and Shen's model and the combined model.

stapes in the oval window[22, 23]. In the otosclerotic ear, the stape is immobilized in the oval window and the cochlea disconnected from the middle ear system[6]. In Zwislocki's and Kringlebotn's models, the value of the impedance at the oval window is infinite, becoming an open circuit at that point[6, 7]. Instead of making it an open circuit, Voss et al. simulated stapes fixation in various degrees by altering the compliance[24].

In the present study, we simulated tympanograms of the otosclerotic ear in the mild and severe conditions. The model structure of the normal ear and mildly otosclerotic ear is illustrated in Fig. 2. The model structure of the severely otosclerotic ear is illustrated in Fig. 5, in which the impedance at the oval window was set to infinity. Values selected for the model parameters are listed in Tab. 5. The upper panel of Fig. 10 shows a series of conductance (G) and susceptance (B) tympanograms from 226 to 1243 Hz calculated from the model of a normal ear. The susceptance (B) tympanograms begin to notch at 791 Hz and the resonant frequency is about 904 Hz. The middle panel of Fig. 10 shows a series of tympanograms calculated from the model of a mildly otosclerotic ear. The susceptance (B) tympanograms begin to notch at 904 Hz and the resonant

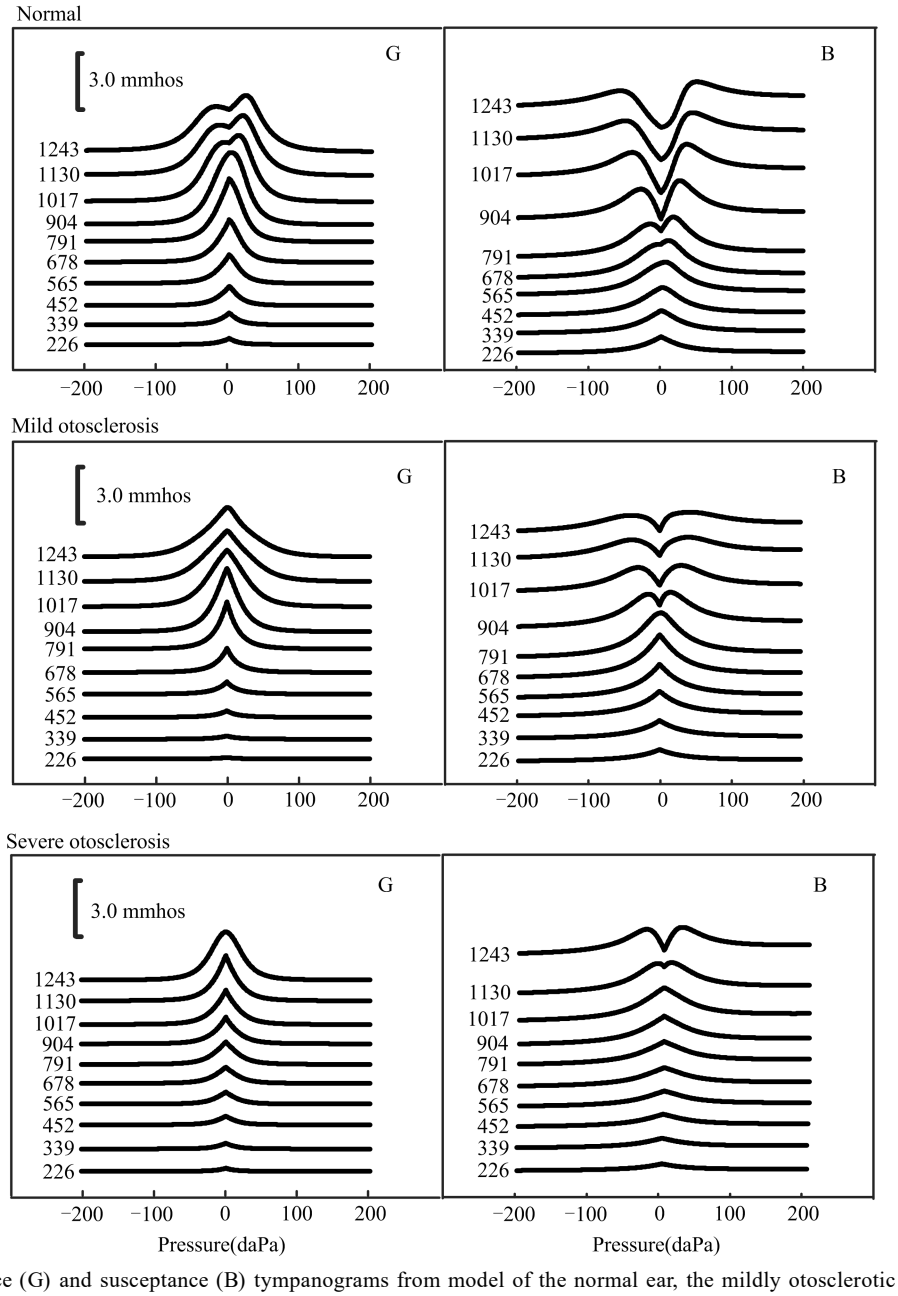

Fig. 10 Conductance (G) and susceptance (B) tympanograms from model of the normal ear, the mildly otosclerotic ear and the severely otosclerotic ear.

frequency is about 1130 Hz. The bottom panel of Fig. 10 shows a series of tympanograms from the model of a severely otosclerotic ear. The susceptance (B) tympanograms begin to notch at 1130 Hz and the resonant frequency is about 1243 Hz. The model results demonstrate that as the degree of otosclerosis increases, the stiffness of the middle ear system increases and consequently the resonant frequency increases.

4 Conclusions

Based on Chen and Shen's computational model, tympanograms under conditions of different middle ear diseases such as otosclerosis and atrophy of tympanic membrane were simulated through manipulating model parameters. And the tympanograms from the model were in agreement with experimental observations. The present study applied Chen and Shen's model to the various types of tympanograms that are typically seen in pathological ears such as otosclerosis and atrophy of tympanic membrane and provided evidence that the model could be suitable for different middle ear diseases. The present study may help to yield explanations for different shapes of tympanograms under conditions of different middle ear diseases and

may help people understand different kinds of tympanograms from a theoretical point of view.

Tab. 4 Parameter values in the combined model selected for simulating tympanograms of the ear with a flaccid eardrum.

Element	Combined model	Unit
Ra	10	Ω
La	29	mH
Cp	5.1	μF
Rm	40	Ω
Ct	0.35	μF
*Rd*1	15	Ω
*Cd*1	1.0	μF
*Rd*2	10	Ω
Cd2	0.8	μF
Ld	25	mH
Ro	245	Ω
Lo	80	mH
Co	2.8	μF
Rs	50	Ω
Cs	0.8	μF
Llksv	5×10^{4}	mH
Rlksv	9.8×10^{5}	Ω
Ldiff	6.46×10^{5}	mH
Rdiff	3.04×10^{5}	Ω
Lrw	1.24×10^{4}	mH
Crw	1.38×10^{-3}	μF
Rrw	6.33×10^{4}	Ω
Lca	5.6×10^{6}	mH
Rca	$3.5\times10^{6}\times\sqrt{f/1kHz}$	Ω

Tab. 5 Parameter values selected for simulating tympanograms of the normal ear, the mildly otosclerotic ear and the severely otosclerotic ear.

Element	Normal	Mild otosclerosis	Severe otosclerosis	Unit
Ra	10	10	10	Ω
La	14	14	14	mH
Cp	5.1	5.1	5.1	μF
Rm	500	500	500	Ω
Ct	0.35	0.35	0.35	μF
*Rd*1	200	200	200	Ω
*Cd*1	0.299	0.299	0.158	μF
*Rd*2	220	220	220	Ω
*Cd*2	0.4	0.4	0.212	μF
Ld	45	45	45	mH
Ro	245	245	245	Ω
Lo	40	40	40	mH
Co	1.4	0.42	0.742	μF
Rs	3000	3000	3000	Ω
Cs	0.25	0.075	0.133	μF
Rc	550	550		Ω
Lc	20	20		mH
Cc	0.6	0.18		μF

Acknowledgements

This work was supported by the National Natural Science Foundation of China(81970886).

Conflict of interest

The authors declare no conflict of interest.

Author information

LI Mugeng is currently pursuing his Master's Degree under the supervision of Prof. Chen Lin at University of Science and Technology of China. His research interests mainly focus on hearing science.

CHEN Lin (corresponding author) received his Ph.D. degree at the Department of Communicative Disorders and Sciences, State University of New York at Buffalo, USA in 1995. He is currently a professor at University of Science and Technology of China. He is interested in research into the central auditory processing under normal and pathological conditions.

References

[1] Chen L, Shen Y H. A computational model for tympanometry. The Journal of the Acoustical Society of America, 1996, 99(6): 3558-3565.

[2] Katz J, Medwetsky L, Buckard R F, et al. Handbook of Clinical Audiology. 7th ed. Philadelphia: Lippincott Wiilliams & Wlikins, 2014.

[3] Lilly D J. Multiple frequency, multiple component tympanometry: new approaches to an old diagnostic problem. Ear and Hearing, 1984, 5(5): 300-308.

[4] Shanks J E. Tympanometry. Ear and Hearing, 1984, 5(5): 268-280.

[5] Vanhuse V J, Creten W L, Camp K J V. On the W-notching of tympanograms. Scandinavian Audiology, 1975, 4(1): 45-50.
[6] Zwislocki J. Analysis of the middle-ear function. part I: input impedance. The Journal of the Acoustical Society of America, 1962, 34(8): 1514-1523.
[7] Kringlebotn M. Network model for the human middle ear. Scandinavian Audiology, 1988, 17(2): 75-85.
[8] Kringlebotn M. Acoustic impedance in the human ear canal. Scandinavian Audiology, 1994, 23(1): 65-71.
[9] Jerger J. Clinical experience with impedance audiometry. Arch Otolaryngol, 1970, 92(4): 311-324.
[10] Han D Y, Zhai S Q, Han W J. Clinical Audiology. 2nd ed. Beijing: Peking Union Medical College Press, 2008. (in Chinese)
[11] Kinsler L E, Frey A R, Coppens A B, et al. Fundamentals of Acoustics. 4th ed. New York: Wiley, 2000.
[12] Shanks J, Shelton C. Basic principles and clinical application of tympanometry. Otolaryngologic Clinics of North America, 1991, 24(2): 299-328.
[13] Zwislocki J. Some impedance measurements on normal and pathological ears. The Journal of the Acoustical Society of America, 1957, 29(12): 1312-1317.
[14] Funasaka S, Funai H, Kumakawa K. Sweep-frequency tympanometry: Its development and diagnostic value. Audiology, 1984, 23(4): 366-379.
[15] Iacovou E, Vlastarakos P V, Ferekidis E, et al. Multi-frequency tympanometry: clinical applications for the assessment of the middle ear status. Indian Journal of Otolaryngology and Head & Neck Surgery, 2013, 65(3): 283-287.
[16] Puria S, Allen J B. Measurements and model of the cat middle ear: Evidence of tympanic membrane acoustic delay. The Journal of the Acoustical Society of America, 1998, 104 (6): 3463-3481.
[17] O'connor K N, Puria S. Middle-ear circuit model parameters based on a population of human ears. The Journal of the Acoustical Society of America, 2008, 123(1): 197-211.
[18] Elliott S J, Ni G, Verschuur C A. Modelling the effect of round window stiffness on residual hearing after cochlear implantation. Hearing Research, 2016, 341(1): 155-167.
[19] Frear D L, Guan X, Stieger C, et al. Impedances of the inner and middle ear estimated from intracochlear sound pressures in normal human temporal bones. Hearing Research, 2018, 367:17-31.
[20] Withnell R H, Gowdy L E. An analysis of the acoustic input impedance of the ear. Journal of the Association for Research in Otolaryngology, 2013, 14(5): 611-622.
[21] Xue L, Liu H, Wang W, et al. The role of third windows on human sound transmission of forward and reverse stimulations: A lumped-parameter approach. The Journal of the Acoustical Society of America, 2020, 147(3): 1478.
[22] Hunter L L, Shahnaz N. Acoustic Immittance Measures Basics and Advanced Practice. San Diego: Plural Publishing, 2014.
[23] Wang S, Hao W, Xu C, et al. A study of wideband energy reflectance in patients with otosclerosis: Data from a Chinese population. Biomed Research International, 2019, 2019:1-8.
[24] Voss S E, Merchant G R, Horton N J. Effects of middle-ear disorders on power reflectance measured in cadaveric ear canals. Ear and Hearing, 2012, 33(2): 195-208.

中耳疾病条件下鼓室导纳测试的理论分析

李牧耕，陈　林*
中国科学技术大学合肥微尺度物质科学国家研究中心,安徽合肥 230027

摘要: 鼓室导纳测试是指改变外耳道压力的同时观测中耳系统声导纳的变化.由于利用鼓室导纳测试评估中耳系统功能具有非侵入性和客观性等优点，它在临床耳鼻喉科中得到了广泛的应用.本工作通过适当调整中耳电路模型中的参数，模拟了鼓膜萎缩、耳硬化症等不同中耳疾病的鼓室导纳图，得到了与典型的临床图像相吻合的模拟图像.我们把最新的内耳电路模型与经典的中耳电路模型相结合，模拟了鼓膜萎缩的鼓室导纳图.将改进的中耳电路模型推广到鼓膜萎缩与耳硬化症等疾病可以进一步帮助人们理解鼓室导纳图形成的机制和促进它在临床中的应用.

关键词: 中耳；鼓室导纳图；耳硬化症；中耳电声模型